Available online at www.sciencedirect.com
SCIENCE DIRECT
Biochimica et Biophysica Acta 1758 (2006) 154–163
BIOCHIMICA ET BIOPHYSICA ACTA
BBA
http://www.elsevier.com/locate/bba

Cell selectivity correlates with membrane-specific interactions: A case study on the antimicrobial peptide G15 derived from granulysin

Ayyalusamy Ramamoorthy [a,*], Sathiah Thennarasu [a,1], Anmin Tan [a], Dong-Kuk Lee [a,2], Carol Clayberger [b], Alan M. Krensky [b]

[a] *Department of Chemistry and Biophysics Research Division, University of Michigan, 930 N. University Avenue, Ann Arbor, MI 48109-1055, USA*
[b] *Division of Immunology and Transplantation Biology, Department of Pediatrics, Stanford University School of Medicine, Stanford, CA 94305, USA*

Received 9 July 2005; received in revised form 8 February 2006; accepted 13 February 2006
Available online 10 March 2006

Abstract

A 15-residue peptide dimer G15 derived from the cell lytic protein granulysin has been shown to exert potent activity against microbes, including *E. coli*, but not against human Jurkat cells [Z. Wang, E. Choice, A. Kaspar, D. Hanson, S. Okada, S.C. Lyu, A.M. Krensky, C. Clayberger, Bactericidal and tumoricidal activities of synthetic peptides derived from granulysin. J. Immunol. 165 (2000) 1486–1490]. We investigated the target membrane selectivity of G15 using fluorescence, circular dichroism and ^{31}P NMR methods. The ANS uptake assay shows that the extent of *E. coli* outer membrane disruption depends on G15 concentration. ^{31}P NMR spectra obtained from *E. coli* total lipid bilayers incorporated with G15 show disruption of lipid bilayers. Fluorescence binding studies on the interaction of G15 with synthetic liposomes formed of *E. coli* lipids suggest a tight binding of the peptide at the membrane interface. The peptide also binds to negatively charged POPC/POPG (3:1) lipid vesicles but fails to insert deep into the membrane interior. These results are supported by the peptide-induced changes in the measured isotropic chemical shift and $T1$ values of POPG in 3:1 POPC:POPG multilamellar vesicles while neither a non-lamellar phase nor a fragmentation of bilayers was observed from NMR studies. The circular dichroism studies reveal that the peptide exists as a random coil in solution but folds into a less ordered conformation upon binding to POPC/POPG (3:1) vesicles. However, G15 does not bind to lipid vesicles made of POPC/POPG/Chl (9:1:1) mixture, mimicking tumor cell membrane. These results explain the susceptibility of *E. coli* and the resistance of human Jurkat cells to G15, and may have implications in designing membrane-selective therapeutic agents.

Keywords: Granulysin; Antimicrobial peptide; Membrane-disruption; Lipid-peptide; NMR; Fluorescence

1. Introduction

Granulysin, a 9-kDa bactericidal protein present in human cytotoxic T cells, disrupts lipid membranes [1,2] and induces apoptosis in mammalian cells [3]. Granulysin exhibits potent cell lytic activity against both Gram-positive and Gram-negative bacteria, fungi, parasites and tumor cells, including *Mycobacterium tuberculosis* and *Mycobacterium leprae* [4]. The MIC value for granulysin against *E. coli* is 1.25 μM [5]. The crystal structure of granulysin revealed the presence of five helical segments held together by two disulfide linkages and resembles other "saposin folds" such as porcine NK-lysin [6], saposins A and C [7], the cyclic peptide bacteriocin AS-48 [8], one domain of prophytepsin [9] and amoebapores [10]. Cys-7 in helix 1 (residues 3–18) and Cys-70 in helix 5 (residues 66–72), and Cys-34 in helix-2 (residues 23–36) and Cys-45 in helix-3 (residues 42–51) are linked by disulfide linkages [11]. The helices are amphipathic and consist of 12 arginine and 3 lysins. To determine the minimum active portion of granulysin protein

Abbreviations: ANS, anilinonaphthalene-8-sulfonic acid; CD, circular dichroism; Chl, cholesterol; H_{II}, inverted hexagonal phase; MIC, minimum inhibitory concentration; MAS, magic angle spinning; NMR, nuclear magnetic resonance; POPC, 1-palmitoyl-2-oleoyl-*sn*-glycero-3-phosphatidylcholine; POPG, 1-palmitoyl-2-oleoyl-*sn*-glycero-3-phosphatidylglycerol; SUVs, small unilamellar vesicles

* Corresponding author. Tel.: +1 734 647 6572; fax: +1 734 763 2307.
E-mail address: ramamoor@umich.edu (A. Ramamoorthy).
[1] Present address: Central Leather Research Institute, Adyar, Chennai-600 020, Tamil Nadu, India.
[2] Present address: Department of Fine Chemistry, Seoul National University of Technology, Seoul, Korea 139-743.

0005-2736/$ - see front matter © 2006 Elsevier B.V. All rights reserved.
doi:10.1016/j.bbamem.2006.02.014

retaining antimicrobial activity, lytic activities of several synthetic peptide fragments derived from granulysin have been investigated [1]. It was shown that helices 2 and 3 are important for the cell lytic activity of granulysin as the peptide G8 corresponding to the helix-2–loop–helix-3 region (residues 23–51) exhibit lytic activities against bacteria and human cells [1,12]. On the other hand, peptides containing either helix 2 or helix 3 lyse bacteria, while only peptides containing helix 3 lyse tumor targets and the peptides corresponding to the amino or carbonyl regions are not lytic. It was also reported that the two positively charged arginines (Arg-38 and Arg-40) in the loop region between helices 2 and 3 are thought to be important for lysis of tumor cells while lysis of human cells is dependent on the helix-3 sequence [1]. While these functional studies are exciting, the details on the peptide–membrane interactions that lead to the lytic activities of these peptides have not been investigated. In this study, we investigate the nature of lipid–peptide interactions, as the differences in the nature of interactions may provide the basis for the development of membrane selective antibiotics.

One of the important peptide fragments, G15, was designed to examine the role of the arginine residues. G15 corresponding to the residues 37–51 of granulysin was synthesized by substituting both the arginine residues (Arg-38 and Arg-40) with glutamine residues. The G15 peptide has been shown to exhibit reduced lytic activity against bacteria and human Jurkat cells [1]. As such, the G15 peptide monomer has 3 cationic charges and shows neither antimicrobial nor antitumor activities. However, under non-reducing conditions, the peptide undergoes dimerization through intermolecular S–S linkage resulting in a 30-residue G15 peptide with 6 cationic charges (Fig. 1).

The purpose of the present study was to understand the specific interactions of G15 with different model membranes, which might form the basis for the cell selective interactions of the peptide. We investigated the *E. coli* outer membrane disruption induced by G15 using the ANS uptake assay. The peptide's ability to permeabilize bacterial inner membrane was studied using ^{31}P and ^{2}H NMR experiments. The intrinsic tryptophan fluorescence was used as a probe to obtain information on the membrane bound peptide. The binding interactions of G15 and peptide-induced dye leakage were investigated using liposomes formed of *E. coli* lipids, POPC/POPG (3:1), and POPC/POPG/Chl (9:1:1) lipid mixtures. In order to offer a more in-depth view on the interaction of G15 with different model membranes mimicking bacterial and tumor cell membranes, the information gathered in the present study will be coupled with the results provided by the on going investigations on different granulysin peptides [1,12,13].

Fig. 1. Amino acid sequence of the peptide dimer G15.

2. Materials and methods

2.1. Materials

POPG, POPC, d_{31}-POPC, and *E. coli* total lipid extract were purchased from Avanti Polar Lipids (Alabaster, AL). Chloroform, cholesterol and methanol were procured from Aldrich Chemical Inc. (Milwaukee, WI). Naphthalene was from Fisher Scientific (Pittsburgh, PA). Buffers were prepared using water obtained from NONApure A filtration system. All the chemicals were used without further purification. The synthesis of the peptide G15 was published elsewhere [1].

2.2. Outer membrane disruption assay

The outer membrane permeabilizing ability of the peptide was investigated using the 1-anilinonaphthalene-8-sulfonic acid (ANS) uptake assay [14,15], using *E. coli* strain BL21 (DE3). Bacterial cells from an overnight culture were inoculated into LB medium. Cells from the mid-log phase were centrifuged and washed with Tris-buffer (10 mM Tris, 150 mM NaCl, pH 7.4), and then resuspended in Tris-buffer to an OD_{600} of 0.065. To a 3.0 mL of the cell suspension in a cuvette, a stock solution of ANS was added to a final concentration of 5.0 μM. The degree of membrane disruption as a function of peptide concentration was observed by the increase in fluorescence intensity at ~500 nm.

2.3. Solid-State NMR

Multilamellar vesicles (MLVs) (or unoriented bilayers) were prepared by mixing the required amounts of lipid and peptide in 2:1 chloroform:methanol. The solution was first dried under N_2 gas and then under vacuum overnight to completely remove any residual organic solvents. The mixture was resuspended in 50 wt.% water by heating in a water bath at 45 °C. The samples were vortexed for 3 min and freeze–thawed using liquid nitrogen several times to obtain a uniform mixture of lipid and peptide. All MLV samples were stored at −20 °C prior to use.

Mechanically aligned POPC/POPG (3:1) and *E. coli* total lipid bilayers were prepared using the procedure described by Hallock et al. [16]. Briefly, 4 mg of lipids and an appropriate amount of peptide were dissolved in $CHCl_3/CH_3OH$ (2:1) mixture. The sample was dried under a stream of nitrogen and re-dissolved in $CHCl_3/CH_3OH$ (2:1) mixture containing equimolar quantities of naphthalene. An aliquot of the solution (~300 μL) was spread on two thin glass plates (11 mm × 22 mm × 50 μm, Paul Marienfeld GmbH and Co., Bad Mergentheim, Germany). The samples were then air-dried and kept under vacuum at 35 °C for at least 15 h to remove naphthalene and any residual organic solvents. After drying, the samples were hydrated at 93% relative humidity using saturated $NH_4H_2PO_4$ solution [17] for 2–3 days at 37 °C, after which approximately 2 μL of H_2O was misted onto the surface of the lipid–peptide film. The glass plates were stacked, wrapped with parafilm, sealed in plastic bags (Plastic Bagmart, Marietta, GA), and then kept at 4 °C for 6–24 h.

All NMR spectra of were obtained from a Varian Infinity 400 MHz solid-state NMR spectrometer operating at resonance frequencies of 400.138, 161.979, and 61.424 MHz for ^{1}H, ^{31}P, and ^{2}H nuclei, respectively. A Chemagnetics temperature controller was used to maintain the sample temperature, and each sample was equilibrated at 30 °C for at least 30 min before the experiment was started. A home-built double resonance probe, which has a four-turn square-coil (12 mm × 12 mm × 4 mm) constructed using a 2-mm wide flat-wire and a spacing of 1 mm between turns, was used for experiments on aligned samples and a triple-resonance MAS probe was used for experiments on MLVs. In the case of aligned samples, the lipid bilayers were positioned in such a way that the bilayer normal was parallel to the external magnetic field of the NMR spectrometer. A typical ^{31}P 90°-pulse length of 3.1 μs was used. ^{31}P spectra were obtained using a spin-echo sequence (90°–τ–180° with τ = 100 μs), 40 kHz rf field for time proportional phase modulation decoupling of protons [18], 50 kHz spectral width, and a recycle delay of 3 s. A typical spectrum required the co-addition of 500–800 transients for aligned samples and about 4000 transients for MLVs. The ^{31}P chemical shift spectra are referenced relative to 85% H_3PO_4 (0 ppm) [16]. A quadrupole echo pulse sequence (90°–τ–90°

with τ=60 μs) was used to acquire the ^{2}H data. Data processing was accomplished using the Spinsight software (Varian) on a Sun Sparc workstation.

2.4. Fluorescence spectroscopy

The steady state fluorescence emission spectra of peptide–vesicle mixtures were measured on a FluoroMax2 spectrofluorimeter (Jobin Yvon-Spex Instruments, S.A. Inc. Edison, NJ). To a 7.8-μM solution of G15 in Tris-buffer (10 mM Tris, 100 mM NaCl, 2 mM EDTA, pH 7.4), increasing amounts of small unilamellar vesicles (SUVs) made of *E. coli* total lipids, POPC/POPG (3:1) or POPC/POPG/Chl (9:1:1) were added and the changes in the fluorescence of the intrinsic tryptophan residue were recorded. Spectra were recorded 5 min after each addition of lipids to allow equilibrium binding. The excitation wavelength was set at 295 nm with a bandwidth of 5 nm. For the red edge excitation shift measurements, the peptide was incubated with POPC/POPG (3:1) liposomes (500 μM) for 60 min to achieve equilibrium binding.

2.5. Dye leakage assay

Carboxyfluorescein dye entrapped SUVs were prepared as described elsewhere [15]. Briefly, Tris-buffer containing 50 mM dye was added to the dry lipid film, vortexed and sonicated. The dye-containing vesicles were then purified by gel filtration chromatography, using a Sephadex G-75 column. To an aliquot of vesicle suspension (60 μM lipid) in Tris-buffer, serial concentrations of peptides were added and the fluorescence emission intensity at 520 nm was recorded as a function of time using the excitation wavelength 490 nm. The maximum leakage from each sample was determined by adding 1% triton X-100.

2.6. Circular dichroism

Small unilamellar vesicles were prepared by sonication. Different lipids in appropriate proportions were dissolved in chloroform and the clear solution was taken to dryness. Tris-buffer was added to dry lipid film and subjected to vortex and sonication to obtain a clear dispersion of SUVs. CD spectra were recorded (AVIV CDS Model 62DS spectropolarimeter, Lakewood, NJ) at 25 °C using samples with a peptide/lipid ratio of about 1:50 in a quartz cuvette (path length=0.1 cm) over the range from 200 to 250 nm. Minor contributions from the buffer and SUVs were removed by subtracting the spectra of the corresponding control sample without peptide. The resultant spectra were normalized for path length and concentration.

3. Results

3.1. Disruption of E. coli membrane

A subset of granulysin peptides corresponding to helix2–loop–helix3 region of granulysin, exhibit potent lytic activities against microbes, red blood cells and human tumor cells [1,5,12]. The peptide G15 shows antimicrobial activity against the Gram-negative bacteria at micromolar concentrations and is slightly less active than the parent peptide granulysin [1]. Since granulysin increases membrane permeability of *E. coli* [5], it is likely that G15 exerts its activity by permeabilizing the bacterial membrane. Therefore, G15-induced bacterial membrane disruption was monitored using ANS uptake assay [14,15]. The ANS (5 μM) equilibrated with *E. coli* cells (OD_{600}=0.0605) showed an emission maximum at ~519 nm (Fig. 2, trace 1). Successive addition of 8 μL (4.3 μM) aliquots of G15 to a 3 mL cell suspension resulted in an enhancement in the fluorescence intensity of ANS and a shift in the emission maximum. At 152 μg/mL peptide concentration, the observed emission maximum was ~510 nm. The blue shift in the emission maximum and the enhancement in the fluorescence intensity of ANS indicate that ANS relocates into a relatively less polar environment, presumably, the bacterial membrane as a consequence of outer membrane disruption by G15. However, ANS showed a blue shifted emission maximum at ~497 nm when 27.7 μg/mL of G8, the cell-lytic antimicrobial peptide derived from granulysin, was used against *E. coli* pretreated with ANS dye (data not given). These results suggest that G15 is a weaker membrane-disrupting agent than the lytic peptide G8.

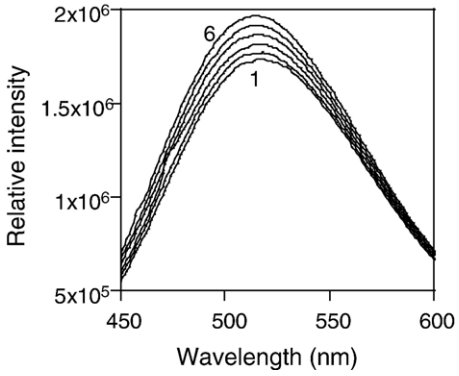

Fig. 2. G15-induced ANS uptake into *E. coli* membranes. Fluorescence spectrum of ANS equilibrated with *E. coli* cells (trace 1), and in the presence of 4.3 μM (trace 2), 8.6 μM (trace 3), 12.9 μM (trace 4) and 17.2 μM (trace 5) and 21.6 μM (trace 6) concentrations of G15. The *E. coli* cell density, as measured at OD_{600}, was 0.065.

Since G15 exhibited a moderate disruption of *E. coli* outer membrane, its ability to disrupt bacterial inner membrane was assessed using model membranes and ^{31}P NMR experiments. Mechanically aligned bilayers formed of *E. coli* lipids gave a broad signal in the range from 22 ppm to 30 ppm with the major component centered at ~25 ppm (Fig. 3). All spectra (with and without the peptide) also show a broad low signal-to-noise ratio signal from 22 ppm to −6 ppm, which could originate from the unoriented part of the sample. On the other hand, *E. coli* lipid bilayers incorporated with G15 show a peak at −10 ppm that increases the intensity with the increase of the peptide concentration from 1 to 5 mol%. Even though some of this signal could be due to the unoriented part of the lipid sample on glass plates, some of this could be due to the formation of a lipid–peptide complex that disorders (either conformationally and/or dynamically) the head group region of lipids. To confirm this observation and interpretation, we repeated the experiments two times on each sample and the spectra were reproducible. In addition, three different samples were prepared for each P:L and the experiments produced identical results for each P:L. Also, from our experience, the aligned samples prepared using the naphthalene procedure are well hydrated, quite stable and the results have been reproducible [16,19–26]; such observations were also reported from another independent study on an antimicrobial peptide [27]. Experimental results on the interaction of the peptide with anionic membrane are given below (Figs. 7 and 8). Therefore, these results show the ability of the peptide to moderately disrupt bacterial inner membrane,

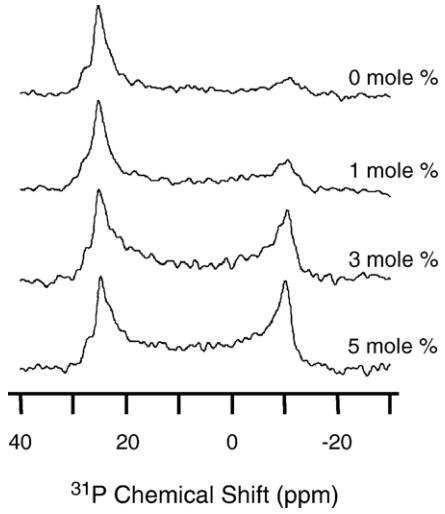

Fig. 3. ^{31}P chemical shift spectra of oriented *E. coli* lipid bilayers in the absence and presence of G15 at 25 °C. The bilayer normal was parallel to the external magnetic field of the spectrometer.

which is consistent with the above-mentioned fluorescence data on the ANS uptake assay.

The consequences of G15 binding to the SUVs formed of *E. coli* lipids were also examined. The fluorescence property of the two tryptophan-residues present in G15 was exploited to assess the binding interactions. The fluorescence emission spectrum of G15 (6.3 μM) dissolved in Tris buffer (pH 7.4) showed an emission maximum at ~354 nm. When aliquots from a 5-mM stock suspension of *E. coli* lipid vesicles were added to the peptide solution, the fluorescence intensity decreased significantly, indicating a tight binding of G15 at the bilayer interface [28]. The peptide-vesicle suspension turned slightly turbid when higher amounts of vesicles were added, suggesting a peptide-induced aggregation of vesicles. Fig. 4 shows the Stern–Volmer plot of the quenching of G15 fluorescence by the SUVs formed of *E. coli* lipids.

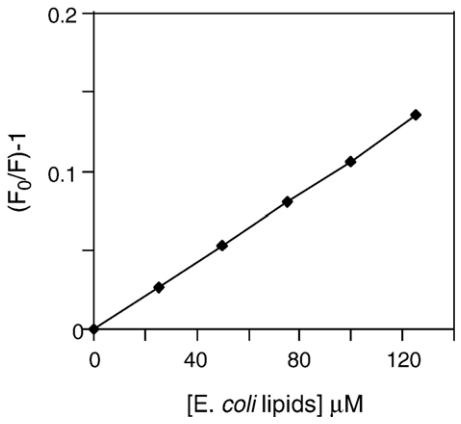

Fig. 4. Stern–Volmer plot derived from the fluorescence quenching of G15 by the addition of *E. coli* total lipid vesicles. Aliquots from a 5-mM stock suspension of lipid vesicles were added to G15 (6.3 μM) in Tris buffer. The intensity of fluorescence at the emission maximum 254 nm was measured after excitation at 295 nm. The excitation and emission bandwidths were kept at 5 nm. F_0 and F are the fluorescence intensities in the absence and presence of lipid vesicles, respectively. For each sample, a blank spectrum was recorded and subtracted from the sample spectrum.

3.2. Interaction with negatively charged membranes

It has recently been shown that the lipid composition of a model membrane modulates peptide activity [21–23,25]. Studies on granulysin protein proposed that the electrostatic interaction between the anionic bacterial inner membrane and the highly positive charged granulysin (there are 15 positively charged residues) would be an important factor in its antimicrobial activity [5]. Therefore, in this study, we investigated the interaction of G15 with model membranes with different compositions to understand the role of an anionic lipid in the activity of G15 and the molecular basis for cell-selective interactions. The trace 1 of Fig. 5 is the steady state fluorescence emission spectrum of G15 (6.3 μM) in Tris buffer (pH 7.4). Addition of aliquots of SUVs (100 μM) to the peptide resulted in an enhancement in the fluorescence intensity and a shift in the emission maximum of G15 (Fig. 5, traces 2–6). As shown in Fig. 6 (trace A), there is a shift towards lower wavelengths in the emission maximum of G15 upon binding to POPC/POPG (3:1) vesicles. These data indicate that G15 binds to negatively charged membranes and that the tryptophan residue relocates into a relatively less polar environment [29].

A polar fluorophore, like tryptophan when present in a viscous medium, exhibits excitation wavelength-dependent fluorescence emission maximum. The difference in the emission maximum after excitation at the red edge of the absorption spectrum is called the red edge excitation shift (REES), and is indicative of a restricted motion of the tryptophan residue [30]. Fig. 6 (trace B) shows the excitation wavelength-dependent shift in the fluorescence emission maximum of tryptophan for G15 bound to POPC/POPG (3:1) liposomes. As shown in Fig. 6, a REES value of 2 nm was observed. The low REES value is in accordance with an interfacial localization of tryptophan residue [31].

Since the G15 peptide is cationic (net charge is +3) and the ^{31}P chemical shift of the lipid is highly sensitive to the charge density on the bilayer surface, the binding of G15 to the bilayers

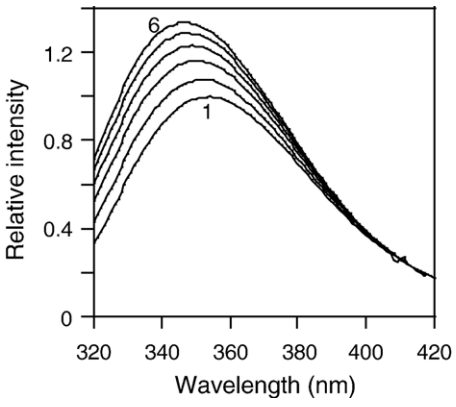

Fig. 5. Fluorescence emission spectra of G15 (6.3 μM) upon binding to (1) 0, (2) 100, (3) 200, (4) 300, (5) 400 and (6) 500 μM of POPC–POPG (3:1) lipid vesicles.

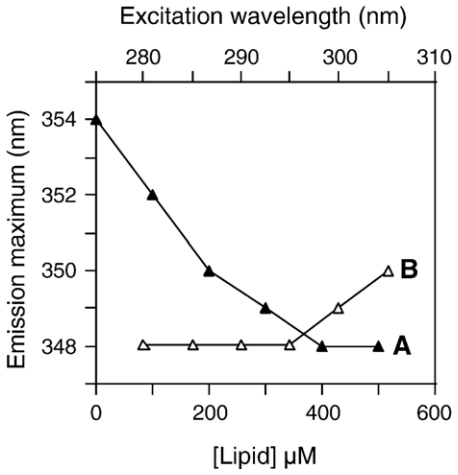

Fig. 6. Blue shift in fluorescence emission maximum of G15 (▲; 6.3 μM) upon binding to POPC–POPG (3:1) vesicles (100, 200, 300, 400 and 500 μM), and REES in the fluorescence emission maximum of G15 (△; 6.3 μM) bound to 500 μM lipid vesicles. The peptide was mixed with POPC–POPG (3:1) vesicles (500 μM) and incubated for 1 h. The lipid/peptide molar ratio was ~80:1. The fluorescence emission spectra of G15 were recorded using various excitation wavelengths ranging from 280 to 305 nm. A bandwidth of 5 nm was used for both emission and excitation. For each sample, a blank spectrum was recorded and subtracted from the sample spectrum.

should alter the observed chemical shift frequency. Experiments performed on well-aligned bilayers at 37 °C showed peptide-induced changes in the ^{31}P chemical shift. A single narrow line at the higher frequency (or the parallel) edge of the powder pattern was observed as reported in our earlier publications (data not shown for pure POPC and pure POPG) [16,19–26]. The ^{31}P chemical shift spectrum of oriented bilayers made of POPC/POPG (3:1) lipids shows two peaks in the range from 25 to 29 ppm, originating from the phosphate groups of POPG and POPC lipids, respectively (Fig. 7). When POPC/POPG (3:1) bilayers are incorporated with 1–5 mol% G15, the two peaks coalesce to give a symmetric peak centered at ~27 ppm. These

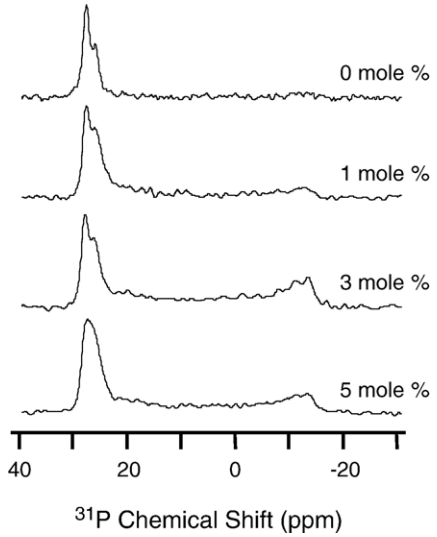

Fig. 7. ^{31}P chemical shift spectra of oriented POPC/POPG (3:1) lipid bilayers in the absence and presence of G15 at 25 °C. The bilayer normal was parallel to the magnetic field.

data suggest that the peptide binding to lipid bilayers affects the conformation of the lipid head group in both POPC and POPG lipids [19–27]. To further confirm these results, ^{31}P NMR experiments were also carried out on static MLVs to measure the peptide-induced changes in the chemical shift span and the line shape. The ^{31}P chemical shift spectra of pure POPC, 3:1 POPC:POPG and POPG MLVs at 37 °C showed typical lamellar phase powder patterns with a chemical shift span of 46±1.5, 38±1.5 and 35±1.5 ppm, respectively. These chemical shift anisotropy values are in good agreement with the reported studies in the literature [32]. The inclusion of G15 peptide (up to 10 mol% peptide) did not show significant observable changes (within experimental errors) in the spectral line shape of POPC bilayers while observable increase in the CSA span was observed in POPG containing bilayers. For example, the CSA span values measured from POPC, 3:1 POPC:POPG and POPG MLVs containing 5 mol% G15 at 37 °C were 47±1.5, 40±1.5 and 38±1.5 ppm, respectively. Sample spectra are shown for 3:1 POPC:POPG bilayers in Fig. 8 (A). On the other hand, increase of peptide concentration to 10 mol% increased the CSA span to 47±1.5 ppm in 3:1 POPC:POPG bilayers. This peptide-induced increase in the CSA is in good agreement with the previous studies on the effect of cations on lipid bilayers [33]. Interestingly, the increase in observed CSA correlates with the increase in the presence of an anionic lipid (that is POPG) in the bilayer suggesting that the peptide G15 preferentially binds

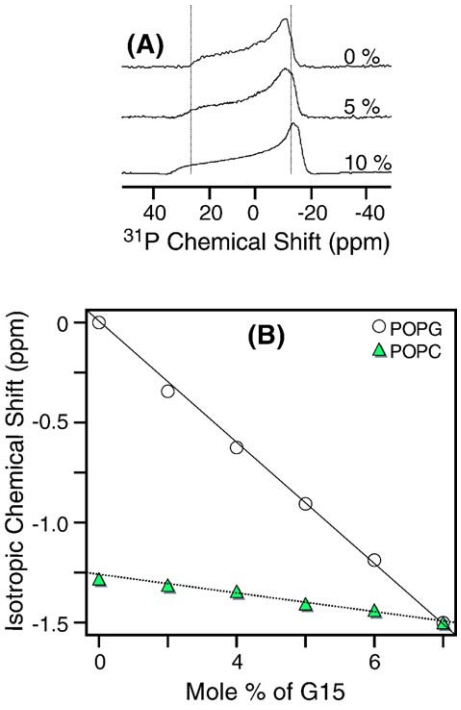

Fig. 8. (A) ^{31}P chemical shift spectra of 3:1 POPC:POPG multilamellar vesicles with different concentrations of G15 peptide (given in mol%). (B) Variation of ^{31}P isotropic chemical shift of 3:1 POPC:POPG multilamellar vesicles under 3±0.005 kHz MAS as a function of the concentration of G15 peptide. The isotropic chemical shift value of POPG (open circles) was set to 0 ppm while that of POPC (filled triangles) was at −1.3 ppm in the absence of the peptide. A 0.25-ppm experimental error in the chemical shift value was measured from the full width at half maximum.

to POPG. These ^{31}P results also suggest that G15 neither promotes the formation of non-lamellar phase structures such as cubic and hexagonal phases nor fragments the MLVs to micelles or SUVs.

In addition to the results obtained from oriented bilayers (Figs. 3 and 7) and static MLVs, magic angle spinning (MAS) ^{31}P NMR experiments were performed on MLVs at 37 °C. Observed spectra contained a narrow line for pure POPC and two narrow lines for 3:1 POPC:POPG separated by about 1.2 ppm (low field peak corresponds to POPG and the high field peak corresponds to POPC) as shown in a recent study on DMPC and DMPG bilayers [33]. The ^{31}P isotropic chemical shift frequency was measured from POPC and 3:1 POPC:POPG bilayers in the presence and absence of G15. While the addition of G15 to POPC bilayers did not alter the ^{31}P peak position, an upfield shift of both the ^{31}P peaks corresponding to POPC and POPG lipids in 3:1 POPC:POPG bilayers was observed. The upfield shift in the isotropic ^{31}P chemical shift value of the POPG is greater than that of the POPC value as shown in Fig. 8B. These results demonstrate that the presence of an anionic lipid (POPG) promotes the binding of the peptide G15 to bilayers and confirm the peptide-induced head group conformation change of POPG lipids. In addition, notable peptide-induced changes were measured in the ^{31}P spin-lattice relaxation ($T1$) values of MLVs at 37 °C under MAS. The addition of 5 mol% peptide slightly increased the $T1$ value from 775±10 to 785±10 ms in POPC bilayers (Table 1). On the other hand, the addition of 5 mol% G15 increased the $T1$ values for both POPC and POPG lipids in 3:1 POPC:POPG bilayers. However, the increase in the $T1$ value of POPG (from 785±10 to 850±10 ms) is significantly larger than that of POPC lipid (from 780±10 ms to 805±10 ms). The increase in $T1$ values in the presence of G15 suggests that the lipid–peptide interaction most likely reduces the axial rotational motion of the lipids, which could make the $T1$ relaxation mechanism less efficient as reported in a recent study [34]. These results further confirm the preference of the peptide to bind with anionic lipids in the bilayer.

A number of antimicrobial peptides that insert into negatively charged vesicles have been reported to induce leakage of vesicular contents [35]. Since G15 interacts with POPC/POPG (3:1) vesicles and disorders the head group region of lipids, its ability to induce dye leakage from lipid vesicles was studied using fluorescence method. Carboxyfluoresceine dye entrapped POPC/POPG (3:1) SUVs (60 μM) were suspended in Tris buffer (pH 7.4) and aliquots of peptide solutions were added. Fig. 9 shows the dye leakage profile upon the addition of G15 (7.8 μM) and G8 (5.5 μM). As shown in Fig. 9, the lytic peptide G8 induces significant dye leakage from POPC/POPG (3:1) vesicles at a lipid to peptide ratio of 11:1, while G15 fails to induce significant dye release even at a lipid to peptide ratio of 8:1.

Table 1
The ^{31}P spin-lattice relaxation, $T1$, values measured from pure and G15-containing multilamellar vesicles using magic angle spinning solid-state NMR experiments at 37 °C

Sample	Lipid	$T1$ for pure lipid	$T1$ for 5 mol% G15
POPC	POPC	775±10	785±10
3:1 POPC:POPG	POPC	785	850
3:1 POPC:POPG	POPC	780	805

The experimental error was 10 ms.

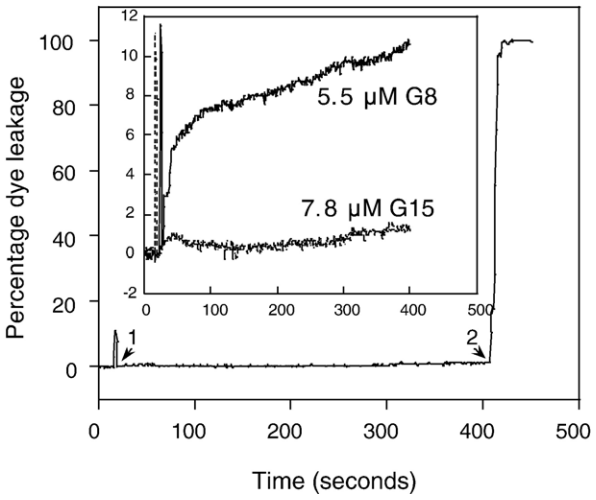

Fig. 9. Peptide induced dye leakage from POPC/POPG (3:1) vesicles. Lipid concentration was 60 μM. The concentration of peptide G15 was 7.8 μM. Arrows 1 and 2 indicate the time of addition of peptide and triton X-100, respectively. Inset shows the blown up image of the initial leakage. The concentration of peptide G8 was 5.5 μM. The hemolytic and antimicrobial peptide G8 was used as a control.

One important component present in mammalian cell membranes is cholesterol (Chl), which is absent in bacterial membranes [36,37]. We examined the equilibrium binding of G15 to vesicles formed from a 9:1:1 mixture of POPC, POPG, and Chl, which approximates the charge characteristics of mammalian tumor cell membrane [38]. Fig. 10 shows the steady state fluorescence spectra of G15 (7.8 μM) in Tris buffer (pH 7.4) and in the presence of 150 μM POPC/POPG/Chl (9:1:1) lipid vesicles; data obtained for 25, 50, 75, 100, and 125 μM POPC/POPG/Chl (9:1:1) lipid vesicles were similar to 150 μM

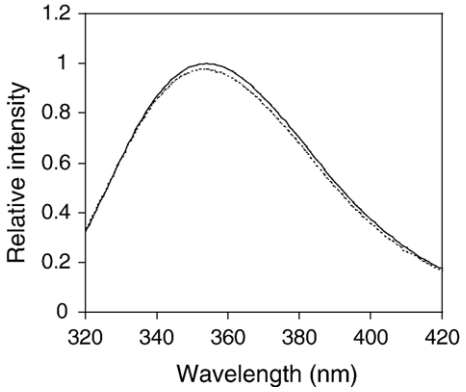

Fig. 10. Fluorescence emission spectra of G15 (7.8 μM) in the absence (solid line) and presence (dashed line) of POPC/POPG/Chl (9:1:1) lipid vesicles (150 μM). The excitation wavelength was 295 nm. Spectra were normalized after subtracting the contributions from buffer and lipid vesicles.

(not shown). The fluorescence intensity of intrinsic tryptophan residue is slightly quenched by the addition of POPC/POPG/Chl (9:1:1) vesicles. Considering the experimental error in these measurements, the observed quenching might indicate a very weak interaction between G15 and POPC/POPG/Chl (9:1:1) vesicles or no interaction at all. To confirm whether the weak interaction leads to leakage of vesicular contents, aliquots of G15 (up to 7.8 μM) were added to SUVs (60 μM) formed of POPC/POPG/Chl (9:1:1) mixture. Peptide G8 was used as a control. While G8 induced ~4% leakage at a concentration of 5.5 μM, G15 failed to cause any significant leakage from POPC/POPG/Chl (9:1:1) vesicles even at concentration of 7.8 μM (data not shown).

3.3. Circular dichroism

Since the interactions of G15 with different types of model membranes were distinct, we studied the secondary structure of the peptide in the presence of different model membranes. The CD spectrum of G15 in aqueous buffer (pH 7.4) exhibited a negative minimum at ~204 nm, suggesting a random coil conformation (Fig. 11). When SUVs made of *E. coli* lipids were added, the suspension turned turbid and hampered CD measurements. These observations appeared as a sign of peptide-induced aggregation of *E. coli* lipid vesicles. However, in the presence of SUVs formed of POPC/POPG (3:1) lipid mixture, the peptide showed a negative minimum at ~206 nm and another shallow negative minimum at ~220 nm, indicating a relatively less ordered conformation, possibly consisting nascent helical turns upon inserting into membrane bilayers. Interestingly, addition of POPC/POPG/Chl (9:1:1) liposomes to the G15 solution did not induce any transitions in the conformation of the peptide. The CD profiles of G15 in buffer and in the presence of POPC/POPG/Chl (9:1:1) vesicles were comparable and omitted for clarity. These observations suggest that the peptide exerts minimal or no perturbations in cholesterol containing lipid vesicles.

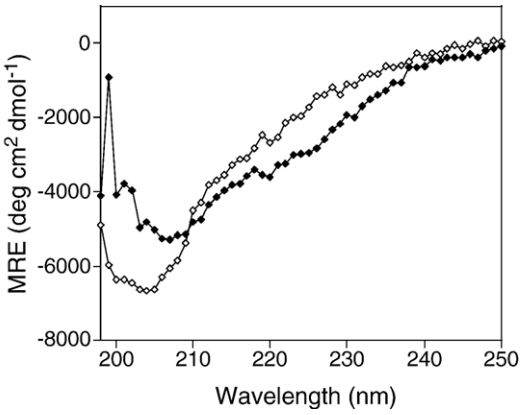

Fig. 11. Circular dichroism spectra of G15 (31.6 μM) in Tris buffer (10 mM Tris, 150 mM NaCl, 2 mM EDTA, pH 7.4), (open diamonds) and POPC/POPG (3:1) lipid vesicles (filled diamonds). Lipid–peptide molar ratio was ~50:1. Spectra were normalized after subtracting the contributions from buffer and lipid vesicles.

4. Discussion

Several antimicrobial peptides bind preferentially to anionic lipids that may form the basis for microbial specificity since bacterial lipid membranes have a net positive charge because of the presence of acidic phospholipids. The significance of specific peptide–lipid interactions has been studied to elucidate the mechanism of antimicrobial action [39]. The mechanisms of cytotoxicity of several antimicrobial peptides have been attributed to their ability to permeabilize the plasma membrane [40]. The differences in the degree of toxicity exerted by these peptides are likely to be associated with the differences in the composition of membranes. Granulysin, and short peptides derived from it, disrupt synthetic liposomes and exhibit activity against bacteria and human Jurkat cells [1,5]. It has been proposed that the mechanism of lysis of bacteria and tumor cells by ganulysin peptides are different [1]. Unlike other granulysin peptides that are also active against tumor cells, G15 does not show any activity against human Jurkat cells [1]. The interesting observation in this study is that the mode of interaction of G15 with different types of model membranes is distinct and differs substantially from each other.

Non-hemolytic cationic peptides have been shown to exhibit potent antimicrobial activity, which could be explained by their potential binding to the negatively charged surface of bacteria [15,39]. In agreement with this assumption, G15 binds to and disrupts *E. coli* outer membrane (Fig. 2) in a concentration dependent manner. However, G15-induced membrane disruption is only marginal when compared with the disruption caused by G8, a cell lytic peptide derived from granulysin. Thus, G15 appears to be a weak membrane-disrupting agent, which is in agreement with its high MIC value against Gram-negative bacteria [1]. Previous research has shown that short antimicrobial peptides that are unable to disrupt bacterial outer membrane destroy the membrane barrier function without pore formation [41,42]. The ability of G15 to induce disorders in bilayers made of *E. coli* total lipids (Fig. 3) suggests a direct interaction of the peptide with bacterial membranes. However, the addition of *E. coli* total lipid vesicles to the peptide solution was accompanied by a reduction in the fluorescence intensity with no blue shift of λ_{max}. This suggests a tight binding of the peptide to the lipid bilayers, a limited insertion of the peptide into the hydrophobic core of the membrane and a possible interaction of tryptophan residues with the phosphate head groups [29].

E. coli lipid mixture contains PE, PG and cardiolipin, out of which PE and cardiolipin have a tendency to form hexagonal phases upon interaction with polycations [20,23,43–45]. These interactions may have a role in the formation of nonbilayer structures such as cubic, hexagonal or micelles. However, the ^{31}P NMR data shown in Figs. 3, 7 and 8A did not show peaks corresponding to non-lamellar phase formation in bilayers and therefore it is unlikely that the G15 peptide functions via non-lamellar phase formation. Thus, neither a 'toroidal' nor a 'barrel stave' mechanism would explain the membrane activity of G15. Given the structure of G15 bound to liposomes, and in aqueous buffer (Fig. 11), a 'carpet' mechanism leading to the formation of local defects in the membrane is a possibility [46].

For short antimicrobial peptides such as G15, it would be intriguing to investigate whether they act by different mechanisms. Our studies indicate that the peptide G15 interacts strongly with POPC/POPG (3:1) and *E. coli* total lipid membranes. However, the mode of interaction with different model membranes is distinct; this is in agreement with the increase in the isotropic chemical shift values (shown in Fig. 8) and the increase in the $T1$ values, which suggested that the peptide prefers to bind with anionic lipid bilayers containing POPG as opposed to a neutral bilayers containing a zwitterionic lipid POPC. These results also suggest that the cationic peptide binding alters the conformation of the lipid head group as reported in the literature [32,33]. While the binding of G15 to *E. coli* lipid vesicles results in the quenching of fluorescence from the intrinsic tryptophan residue, binding to POPC/POPG (3:1) liposomes is followed by an increase in the quantum yield of tryptophan. A shift in the emission maximum from 354 nm to 348 nm was also observed, and is in agreement with the insertion of tryptophan residue and possibly the hydrophobic side chains into POPC/POPG (3:1) bilayers. A blue shift of 6 nm and a REES value of 2 nm in the λ_{max} of tryptophan (Fig. 6) suggest that the tryptophan residue is located at the bilayer interface and not deep inside the hydrophobic region of the membrane [29,47,48]. This assumption is supported by the peptide's inability to induce significant dye-leakage from vesicles formed of POPC/POPG (3:1) mixture (Fig. 9). Inhibition of leakage from anionic liposomes has been previously reported for cationic peptides melittin, nisin, and mastoparan and for the synthetic peptide KLAL [47–50]. Moreover, incorporation of G15 into POPC/POPG (3:1) bilayers does not result in substantial disintegration or micellization of the membrane (both unoriented MLVs and oriented bilayers) (Figs. 3 and 7). Thus, solubilization of membrane bilayers through a detergent-like mechanism is ruled out due to the absence of any isotropic signal in the ^{31}P NMR spectra of the peptide incorporated bilayers formed of POPC/POPG (3:1) mixture as well as *E. coli* total lipids (Figs. 3 and 7). These results are in agreement with recent NMR studies on the interaction of antimicrobial peptides with lipid bilayers [19–27,51–58].

Whereas the fluorescence properties of the intrinsic tryptophan residue are affected by the presence of vesicles formed of *E. coli* lipids and POPC/POPG (3:1) mixture, relatively insignificant changes are observed when vesicles made of POPC/POPG/Chl (9:1:1) mixture are added to the peptide solution (Fig. 11). This clearly suggests that G15 does not insert into POPC/POPG/Chl (9:1:1) membrane. Presence of 3–9% phosphatidylserine makes cancer cell membranes negatively charged [36]. We evaluated the effect of G15 on liposomes formed of POPC/POPG/Chl (9:1:1) mixture, which approximates the charge characteristics of cancer cell membrane. Previous studies have demonstrated that incorporation of cholesterol imparts rigidity to the membrane and weakens the interaction between the peptides and membrane [19,20,59–61]. In our experiments, the reduction in negative charge (low POPG content) and an increase in membrane rigidity (incorporation of cholesterol) may have limited the binding of G15 to liposomes made of POPC/POPG/Chl (9:1:1) mixture. Accordingly, the peptide does not induce any dye leakage from liposomes made of POPC/POPG/Chl (9:1:1) (data not shown). Thus, the inability of the peptide to bind and perturb POPC/POPG/Chl (9:1:1) membrane could account for the peptide's inability to lyse human Jurkat cells.

Several strategies have been used to improve antimicrobial activity and cell selectivity of synthetic peptides. They include: fatty acylation of synthetic peptides, cyclization of linear peptides, substitution of unusual amino acids, and total or partial replacement by D-amino acids. Dimerization of magainin 2 has been shown to exhibit improved activity against various microorganisms and synthetic liposomes [62]. Our study also shows that dimerization through disulfide bond formation could possibly be used as a strategy to impart antimicrobial activity and cell selectivity.

Acknowledgments

This research was supported by funds from the NIH (AI054515 to A. R.). The authors thank Kazutoshi Yamamoto and Dr. Vishnu Dhople for help with some of the experiments in this study.

References

[1] Z. Wang, E. Choice, A. Kaspar, D. Hanson, S. Okada, S.C. Lyu, A.M. Krensky, C. Clayberger, Bactericidal and tumoricidal activities of synthetic peptides derived from granulysin, J. Immunol. 165 (2000) 1486–1490.
[2] D.A. Hanson, A.A. Kaspar, F.R. Poulain, A.M. Krensky, Biosynthesis of granulysin, a novel cytolytic molecule, Mol. Immunol. 36 (1999) 413.
[3] S. Gamen, D.A. Hanson, A. Kaspar, J. Naval, A.M. Krensky, A. Anel, Granulysin-induced apoptosis: I. Involvement of at least two distinct pathways, J. Immunol. 161 (1998) 1758.
[4] J. Kumar, S. Okada, C. Clayberger, A.M. Krensky, Granulysin: a novel antimicrobial, Expert Opin. Investig. Drugs 10 (2001) 321–329.
[5] W.A. Ernst, S. Thoma-Uszynski, R. Teitelbaum, C. Ko, D.A. Hanson, C. Clayberger, A.M. Krensky, M. Leippe, B.R. Bloom, T. Ganz, R.L. Modlin, Granulysin, a T cell product, kills bacteria by altering membrane permeability, J. Immunol. 165 (2000) 7102–7108.
[6] E. Liepinsh, M. Andersson, J.-M. Ruysschaert, G. Otting, Saposin fold revealed by the NMR structure of NK-lysine, Nat. Struct. Biol. 4 (1997) 793–795.
[7] X. Qi, G.A. Grabowski, Differential membrane interactions of saposins A and C: implications for the functional specificity, J. Biol. Chem. 276 (2001) 27010–27017.
[8] C. Gonzalez, G.M. Langdon, M. Bruix, A. Galvez, E. Valdivia, M. Maqueda, M. Rico, Bacteriocin AS-48, a microbial cyclic polypeptide structurally and functionally related to mammalian NK-lysin, Proc. Natl. Acad. Sci. U. S. A. 97 (2000) 11221–11226.
[9] J. Kervinen, G.J. Tobin, J. Costa, D.S. Waugh, A. Wlodawer, A. Zdanov, Crystal structure of plant aspartic proteinase prophytepsin: inactivation and vacuolar targeting, EMBO J. 18 (1999) 3947–3955.
[10] H. Bruhn, M. Leippe, Comparative modeling of amoebapores and granulysin based on the NK-lysin structure: structure and functional implications, Biol. Chem. 380 (1999) 1001–1007.
[11] D.H. Anderson, M.R. Sawaya, D. Cascio, W. Ernst, R. Modlin, A. Krensky, D. Eisenberg, Granulysin crystal structure and a structure-derived lytic mechanism, J. Mol. Biol. 325 (2003) 355–365.
[12] O. Li, C. Dong, A. Deng, M. Katsumata, A. Nakadai, T. Kawada, S. Okada, C. Clayberger, A.M. Krensky, Hemolysis of erythrocytes by granulysin-derived peptides but not by granulysin, Antimicrob. Agents Chemother. 49 (2005) 388–397.

[13] S. Thennarasu, C. Clayberger, A. Ramamoorthy, Membrane Permeabilization of Granulysin Peptides: NMR and Fluorescence study. 36th ACS Central Regional Meeting, IUPUI, Indianapolis, 2004, p. 7 (June 2–4, Abstract #258).
[14] J. Slavik, Anilinonaphthalene sulfonate as a probe of membrane composition and function, Biochim. Biophys. Acta 694 (1982) 1–25.
[15] S. Thennarasu, D-K. Lee, A. Tan, U.P. Kari, A. Ramamoorthy, Antimicrobial activity and membrane selective interactions of a synthetic lipopeptide MSI-843, Biochim. Biophys. Acta 1711 (2005) 49–58.
[16] K.J. Hallock, K.H. Wilderman, D-K. Lee, A. Ramamoorthy, An innovative procedure using a sublimable solid to align lipid bilayers for solid-state NMR studies, Biophys. J. 82 (2002) 2499–2503.
[17] E.W. Washburn, C.J. West, C. Hull, International Critical, Tables of Numerical Data, Physics, Chemistry, and Technology, McGraw-Hill, New York, 1926.
[18] A.E. Bennett, C.M. Rienstra, M. Auger, K.V. Lakshmi, R.G. Griffin, Heteronuclear decoupling in rotating solids, J. Chem. Phys. 103 (1995) 6951–6958.
[19] K.J. Hallock, D-K. Lee, J. Omnaas, H.I. Mosberg, A. Ramamoorthy, Membrane composition determines Pardaxin's mechanism of lipid bilayer disruption, Biophys. J. 83 (2002) 1004–1013.
[20] K.A.H. Wildman, D.K. Lee, A. Ramamoorthy, Mechanism of lipid bilayer disruption by the human antimicrobial peptide, LL-37, Biochemistry 42 (2003) 6545.
[21] K.J. Hallock, D.K. Lee, A. Ramamoorthy, MSI-78, an analogue of the magainin antimicrobial peptides, disrupts lipid bilayer structure via positive curvature strain, Biophys. J. 84 (2003) 3052–3060.
[22] F. Porcelli, B. Buck, D.K. Lee, K.J. Hallock, A. Ramamoorthy, G. Veglia, Structure and orientation of pardaxin determined by NMR experiments in model membranes, J. Biol. Chem. 279 (2004) 45815–45823.
[23] A. Mecke, D.K. Lee, A. Ramamoorthy, B.G. Orr, M.M.B. Holl, Synthetic and natural polycationic polymer nanoparticles interact selectively with fluid-phase domains of DMPC lipid bilayers, Langmuir 21 (2005) 8588–8590.
[24] A. Mecke, D.K. Lee, A. Ramamoorthy, B.G. Orr, M.M.B. Holl, Membrane thinning due to antimicrobial peptide binding: an atomic force microscopy study of MSI-78 in lipid bilayers, Biophys. J. 99 (2005) 4043–4050.
[25] S. Thennarasu, D.K. Lee, A. Poon, K.E. Kawulka, J.C. Vederas, A. Ramamoorthy, Membrane permeabilization, orientation, and antimicrobial mechanism of subtilosin A, Chem. Phys. Lipids 137 (2005) 38–51.
[26] C.D. Pointer-Keenan, D.K. Lee, K.J. Hallock, A. Tan, R. Zand, A. Ramamoorthy, Investigation of the interaction of myelin basic protein with phospholipid bilayers using solid-state NMR spectroscopy, Chem. Phys. Lipids 132 (2004) 47–54.
[27] J.J. Buffy, M.J. McCormick, S. Wi, A. Waring, R.I. Lehrer, M. Hong, Selective perturbation of lipid membranes by the cyclic antimicrobial peptide RTD-1 investigated by solid-state NMR, Biochemistry 43 (2004) 9800–9812.
[28] N. Ben-Tal, B. Honig, R.M. Peitzsch, G. Denisov, S. McLaughlin, Binding of small basic peptides to membranes containing acidic lipids: theoretical models and experimental results, Biophys. J. 71 (1996) 561–575.
[29] B. Christiaens, S. Symoens, S. Vanderheyden, Y. Engelborghs, A. Joliot, A. Prochiantz, J. Vandekerckhove, M. Rosseneu, B. Vanloo, Tryptophan fluorescence study of the interaction of penetratin peptides with model membranes, Eur. J. Biochem. 269 (2002) 2918–2926.
[30] A.P. Demchenko, A.S. Ladokhin, Red-edge-excitation fluorescence spectroscopy of indole and tryptophan, Eur. Biophys. J. 15 (1988) 369–379.
[31] D.J. Schibli, R.F. Epand, H.J. Vogel, R.M. Epand, Tryptophan-rich antimicrobial peptides: comparative properties and membrane interactions, Biochem. Cell Biol./Biochim. Biol. Cell. 80 (2002) 667–677.
[32] J.S. Santos, D.K. Lee, A. Ramamoorthy, Effects of antidepressants on the conformation of phospholipid headgroups studied by solid-state NMR, Magn. Reson. Chem. 42 (2004) 105–114.
[33] F. Lindstrom, P.T.F. Williamson, G. Grobner, Molecular insight into the electrostatic membrane surface potential by $^{14}N/^{31}P$ MAS NMR spectroscopy: nociceptin–lipid association, J. Am. Chem. Soc. 127 (2005) 6610–6618.
[34] J.X. Lu, K. Damodaran, J. Blazyk, G.A. Lorigan, Solid-state nuclear magnetic resonance relaxation studies of the interaction mechanism of antimicrobial peptides with phospholipid bilayer membranes, Biochemistry 44 (2005) 10208–10217.
[35] D. Rapaport, S. Nir, Y. Shai, Capacities of pardaxin analogues to induce fusion and leakage of negatively charged phospholipid vesicles are not necessarily correlated, Biochemistry 33 (1994) 12615–12624.
[36] C.L. Randle, P.W. Albro, J.C. Dittmer, The phosphoglyceride composition of Gram-negative bacteria and the changes in composition during growth, Biochim. Biophys. Acta 187 (1969) 214–220.
[37] A.J. Verkleij, R.F. Zwaal, B. Roelofsen, P. Comfurius, D. Kastelijn, L. V. Deenen, The asymmetric distribution of phospholipids in the human red cell membrane. A combined study using phospholipases and freeze-etch electron microscopy, Biochim. Biophys. Acta 323 (1973) 178–193.
[38] R.F. Zwaal, A.J. Schroit, Pathophysiologic implications of membrane phospholipid asymmetry in blood cells, Blood 89 (1997) 1121–1132.
[39] K. Matsuzaki, Why and how are peptide–lipid interactions utilized for self defence? Biochem. Soc. Trans. 29 (2001) 598–601.
[40] Y. Shai, Mechanism of the binding, insertion and destabilization of phospholipid bilayer membranes by alpha-helical antimicrobial and cell non-selective membrane-lytic peptides, Biochim. Biophys. Acta 1462 (1999) 55–70.
[41] Z. Oren, J. Hong, Y. Shai, A repertoire of novel antibacterial diastereomeric peptides with selective cytolytic activity, J. Biol. Chem. 272 (1997) 14643–14649.
[42] B. Bechinger, The structure, dynamics and orientation of antimicrobial peptides in membranes by solid-state NMR spectroscopy, Biochim. Biophys. Acta 1462 (1999) 157–183.
[43] J.A. Killian, M.C. Koorengevel, J.A. Bouwstra, G.S. Gooris, W. Dowhan, B. de Kruijff, Effect of divalent cations on lipid organization of cardiolipin isolated from *Escherichia coli* strain AH930, Biochim. Biophys. Acta 1189 (1994) 225–232.
[44] A. Schank, M. Deleers, ^{31}P NMR study of the parameters influencing the formation of non-bilayer phases in model membrane, Biochem. Biophys. Res. Commun. 195 (1993) 654–658.
[45] A.M. Batenburg, J.C.L. Hibbeln, A.J. Verkleij, B. de Kruijff, Melittin induces HII phase formation in cardiolipin model membranes, Biochim. Biophys. Acta 903 (1987) 142–154.
[46] M. Wu, E. Maier, R. Benz, R.E.W. Hancock, Mechanism of interaction of different classes of cationic antimicrobial peptides with planar bilayers and with the cytoplasmic membrane of *Escherichia coli*, Biochemistry 38 (1999) 7235–7242.
[47] M.C. Tory, A.R. Merrill, Determination of membrane protein topology by red-edge excitation shift analysis: application to the membrane-bound colicin E1 channel peptide, Biochim. Biophys. Acta 1564 (2002) 435–448.
[48] T. Benachir, M. Lafleur, Study of vesicle leakage induced by melittin, Biochim. Biophys. Acta 1235 (1995) 452–460.
[49] M.J.G. Garcera, M.G.L. Elferink, A.J.M. Driessen, W.W. Konings, In vitro pore-forming activity of the lantibiotic nisin. Role of protonmotive force and lipid composition, Eur. J. Biochem. 212 (1993) 417–422.
[50] N.G. Park, Y. Yamato, S. Lee, G. Sugihara, Interaction of mastoparan-B from venom of a hornet in Taiwan with phospholipid bilayers and its antimicrobial activity, Biopolymers 36 (1995) 793–801.
[51] J.P.S. Powers, A. Tan, A. Ramamoorthy, R.E.W. Hancock, Solution structure and interaction of the antimicrobial polyphemusins with lipid membranes, Biochemistry 44 (2005) 15504–15513.
[52] E. Strandberg, A.S. Ulrich, NMR methods for studying membrane-active antimicrobial peptides, Conccpts Magn. Reson. 23 (2004) 89–120.
[53] S. Abu-Baker, X.Y. Qi, J. Newstadt, G.A. Lorigan, Structural changes in a binary mixed phospholipid bilayer of DOPG and DOPS upon saposin C interaction at acidic pH utilizing P-31 and H-2 solid-state NMR spectroscopy, BBA. Biomembranes 1717 (2005) 58–66.
[54] P.C. Dave, E. Billington, Y.L. Pan, S.K. Straus, Interaction of alamethicin with ether-linked phospholipid bilayers: oriented circular dichroism, P-31

solid-state NMR, and differential scanning calorimetry studies, Biophys. J. 89 (2005) 2434–2442.
[55] I. Marcotte, K.L. Wegener, Y.H. Lam, B.C.S. Chia, M.R.R. de Planque, J.H. Bowie, M. Auger, F. Separovic, Interaction of antimicrobial peptides from Australian amphibians with lipid membranes, Chem. Phys. Lipids 122 (2003) 107–120.
[56] R. Mani, J.J. Buffy, A.J. Waring, R.I. Lehrer, M. Hong, Solid-state NMR investigation of the selective disruption of lipid membranes by protegrin-1, Biochemistry 43 (2004) 13839–13848.
[57] R. Mani, A.J. Waring, R.I. Lehrer, M. Hong, Membrane-disruptive abilities of beta-hairpin antimicrobial peptides correlate with conformation and activity: a P-31 and H-1 NMR study, BBA. Biomembranes 1716 (2005) 11–18.
[58] B. Bechinger, Detergent-like properties of magainin antibiotic peptides: a P-31 solid-state NMR spectroscopy study, BBA. Biomembranes 1712 (2005) 101–108.
[59] G. van Ginkel, H. van Langen, Y.K. Levine, The membrane fluidity concept revisited by polarized fluorescence spectroscopy on different model membranes containing unsaturated lipids and sterols, Biochimie 71 (1989) 23–32.
[60] P.R. Cullis, P.W.M. van Dijck, B. de Kruijff, J. de Gier, Effects of cholesterol on the properties of equimolar mixtures of synthetic phosphatidylethanolamine and phosphatidylcholine. A ^{31}P NMR and differential scanning calorimetry study, Biochim. Biophys. Acta 513 (1978) 21–30.
[61] R.F. Epand, A. Ramamoorthy, R.M. Epand, Membrane lipid composition and the interaction with Pardaxin: the role of cholesterol, Protein Pept. Lett. 13 (2006) 1–5.
[62] C.E. Dempsey, S. Ueno, M.B. Avison, Enhanced membrane permeabilization and antibacterial activity of a disulfide-dimerized magainin analogue, Biochemistry 42 (2003) 402–409.